The Zeno (Z=1) Behavior of Water:

A Molecular Simulation Study [1]

M. T. Reagan[2] and J. W. Tester[2,3]

ABSTRACT

The regularity of fluid properties observed at the Zeno or $Z=PV/RT=1$ point has been proposed as a means of testing and improving volumetric equations of state. Previous research has shown that molecular interactions can be qualitatively and quantitatively related to the linear $Z=1$ contour of T_r vs. ρ_r for pure fluids from the Boyle temperature to the triple point. In this study, we expand the molecular simulation analysis of previous work to gain a detailed microscopic understanding of the properties of Zeno-point systems. Our calculations show that popular semi-empirical water models, such as SPC and SPC/E water, are able to closely replicate experimentally-determined water properties in the Zeno point region. Detailed molecular dynamics simulations of $Z=1.00$ and adjacent $Z=0.75$ and $Z=1.25$ states reveal common features over a wide range of temperatures and densities from 77°C to 1097°C and 1.01 g/cm^3 to 0.029 g/cm^3. Radial distribution functions of high-temperature, high-density Zeno-point fluids display remarkable long-range structural correlation well above the critical temperature and pressure, and examination of hydrogen bonding within each system shows that large water-water hydrogen-bonded clusters persist at high temperatures and supercritical densities. These results are compared to the existing extended corresponding-states approaches for pure fluid properties.

KEYWORDS: hydrogen bonding; molecular simulation; supercritical water; water; Zeno point

1. INTRODUCTION

Researchers have long recognized and studied the regular properties of fluids using unifying concepts such as the Theorem of Corresponding States and the Law of Rectilinear Diameters. Recent investigations [1, 2] have examined another empirical regularity called the *Zeno line*. When the compressibility factor $Z=1$, usually thought of as representing and ideal gas state, one observes that a common contour of states from the gaseous, low-pressure Boyle point to nearly solid densities where the reduced density of many fluids is found to be a linear function of temperature.

The properties of the Zeno point are described in previous work by Herschbach and Ben-Amotz [1, 2] and a recent investigation by this group[3]. At low densities, the $Z=1$ contour is linear in a T vs. ρ plot, with the $\rho \rightarrow 0$ intercept specified by the Boyle temperature. The slope of the contour can be given as the ratio of the third virial coefficient to the derivative of the second, $-B_3/(dB_2/dT)$, evaluated at the Boyle temperature. The most notable feature, however, is that the $Z=1$ contour maintains its linearity in the dense fluid region. It has been suggested that, near the triple point, attractive and repulsive forces balance, compensating for the strong intermolecular forces that would otherwise drive Z away from unity. The Zeno line phenomenon has been found to extend to a wide range of fluids well beyond the realm of standard Corresponding States, with strong correlations to the line of rectilinear diameters from subcritical to supercritical conditions[1, 2]. The T and ρ intercepts of the Zeno line have been found to be strongly correlated with the acentric factors of normal fluids.[4]

The unique properties of Zeno behavior lends itself to novel applications in the area of equation of state (EOS) conception, development, and parameter regression [3, 5]. However, the interesting physical and molecular properties suggested in early work by Herschbach and collaborators demand an in-depth study of not only the macroscopic but the microscopic, molecular-level properties of Zeno-point systems. In this work, we examine the Zeno point behavior of water through a molecular dynamics approach, examining properties, structure, hydrogen bonding, and clustering behavior as represented by simple semi-empirical potential models.

2. SIMULATION METHODOLOGY

In this study, we represent water using the Simple Point Charge (SPC) model of Berendson, *et al* [6]. The SPC model captures both short-range dispersion and long-range Coulombic interactions using pairwise potentials. The Lennard-Jones potential is centered on the oxygen site, with a well depth of $\varepsilon=0.648$ kJ/mol and a diameter of $\sigma=0.3166$ nm. For the standard SPC model, point charges of $-0.82e$ on the oxygen center and $+0.41e$ on each hydrogen site interact through pairwise Coulombic potentials to represent the permanent dipole of water at 2.22 D.

Although the SPC model captures many important properties of pure water, it overestimates other properties such as the self-diffusion coefficient and underestimates the critical temperature. To address these issues, we also employed the modified SPC/E (Extended Simple Point Charge) model, which uses the SPC structural model geometry but increases the magnitude of the point charges to $-0.8476e$ for oxygen and $+0.4238e$ for

hydrogen. The SPC/E model results in a higher permanent dipole of 2.35 D, and critical

properties much closer to those of real water [7].

For each state point of interest, we used 256 SPC or SPC/E water molecules in a

periodic cubic box. To converge on selected value of Z, we used isothermal/isobaric

molecular dynamics with a Nosé-Anderson approach [8, 9] to equilibrate to the specified

value of Z to within ±0.01.   System equilibration was checked by dividing the simulation

into 5,000 cycle blocks to check the evolution of statistics over time. Equilibration runs of

50 to150 ps (50 to 150×10^{-12} s) preceded each 250 to 500 ps production run.using time

steps of 3 to 5 fs.

Several structural quantities were examined for each simulated state point. Radial

distribution functions, $g(r)$, were calculated from 2,000 or more sample configurations

drawn from each production run. In addition, the degree of hydrogen bonding was

estimated using the combined distance-energy criteria of Kalinchev [10, 11]. Using the

knowledge of specific hydrogen-bonded links between molecules, we were also able to

calculate cluster size distributions for selected state points using a Markov chain

formulation of the connectivity matrix, as reported in a previous paper[3].

3. RESULTS

To examine the Zeno line itself, and to confirm that simple, semi-empirical models

can capture the intermolecular properties that drive this effect, seven states points along the

Z=1 contour were modeled with the SPC and SPC/E models. Sample equilibrium

configurations for each SPC run, published in a previous study [3], are shown in Figure 1.

Table 1 contains the equilibrium temperature, pressure, and density of each SPC and SPC/E simulated Z=1 point [3]. Note that despite the commonality of the Z=1 condition, these state points extend over a range of densities from 1.01 g/cm^3 to 0.029 g/cm^3, from subcritical liquid and subcritical vapor to supercritical vapor.

Figure 2 shows the Zeno lines generated by the molecular dynamics simulations [3]. Reduced properties were calculated using the critical properties of each model to maintain consistency—$T_{c,\text{SPC}}$=314 $^\text{o}$C and $\rho_{c,\text{SPC}}$=0.27 g/cm^3, $T_{c,\text{SPC/E}}$=378.6 $^\text{o}$C and $\rho_{c,\text{SPC/E}}$=0.326 g/cm^3.[7, 12] Over a range of reduced density from 0.1 through 3.5, molecular simulation generated straight Zeno lines with slopes of –0.47±0.04 for SPC and –0.45±0.04 for SPC/E. A Z=1 contour generated from experimentally-correlated steam table data [13] is presented for comparison, with a slope of –0.58±0.04. The simulated Zeno lines exhibit excellent linearity, and show good agreement over the full range of density. It is worth noting that the SPC model, fit to ambient water properties, best matches the experimental Boyle temperature for water, while SPC/E water shows improved performance at lower densities and higher temperatures.

Structure at the Zeno Point

A structural analysis of the Z=1 contour reveals the progression of fluid properties from liquid to vapor conditions. Figure 3 shows the radial distribution functions, $g(r)$, for the six Z=1 points calculated with the SPC model, plus the $g(r)$ of ambient water for comparison. Vertical dotted lines indicate r=0.45 nm and r=0.6 nm, the approximate location of the second peak and second minimum for ambient water. As expected, the

amplitude of the RDFs decreases with decreasing density, indicating reduced pairwise correlation. Comparison of the ambient RDF to the $Z=1$ structures shows a shift in the location of the second peak away from 0.45 nm, characteristic of tetrahedral coordination, toward a 0.6 nm position consistent with dodecahedral coordination in the second solvation shell.

To further highlight the long-range structure, we can scale $g(r)$ to remove the inherent density dependence. We define a new, arbitrary function:

$$g_{O-O}^{*}(r) \equiv \frac{h_{O-O}(r)}{\rho} + 1$$

where $h_{O-O}(r) \equiv g_{O-O}(r)-1$. Scaling the direct correlation function with density enhances the structural elements of $g_{O-O}(r)$ of each state point. The scaled radial distribution functions for the same six $Z=1$ points are shown in Figure 4. Once density-related effects are normalized, the structure of the six points is remarkably similar. In particular, the low-density, high-temperature states indicate the presence of second and third shell correlation that one would not expect to see in such energetic vapor-like forms. The enhancement of the peaks further reveals the shift in the position of the second solvation shell from tetrahedral to dodecahedral coordination.

Hydrogen Bonding at the Zeno Point

The properties of the system can also be examined in terms of hydrogen bonding. Using the Kalinchev distance-energy criteria to define water-water hydrogen bonds, we can quantify the degree of hydrogen bonding in terms of the average number of hydrogen bonds per molecule [10]. Figure 5 gives $<n_{hb}>$ vs. T for each of the $Z=1$ points for SPC water.

The graph also includes $<n_{hb}>$ for ambient water and supercritical water at 450 °C and 250 bar, calculated by the same method, as well as a horizontal line demarcating the percolation threshold of 1.56. The degree of hydrogen bonding calculated by the distance-energy method is compared to the structural hydration number calculated by integrating the O-H RDF, $g_{O-H}(r)$, over the first peak without energy consideration. The $Z=1$ state points below 400 °C exhibit a strong deviation from simple structural coordination, indicating that hydrogen-bonded coordination is significant above the percolation threshold and that water clusters must include bonded and non-bonded water molecules in nearest-neighbor positions.

Non-Zeno Contours

The properties of off-Zeno, or $Z \neq 1$, points also merit examination. Figure 6 shows the experimental $Z=0.75$, $Z=1.00$, and $Z=1.25$ contours [13] in comparison with state points modeled with SPC water. We see the same strong correlation between the model properties and experiment, with the deviation decreasing at lower densities. Hydrogen bonding statistics for $Z=0.75$, 1.00, 1.25 points are indicated in Table 2. We see that variation in $<n_{hb}>$ is a function of both the compressibility and density of the fluid. Despite this wide range in the degree of hydrogen bonding within a given Z contour, radial distribution functions for each of these simulated off-Zeno state points look essentially identical in scaled or unscaled form, with only small variations in the height and width of the first peak of $g(r)$ that correlate to system density. The position and magnitude of the second and third peaks do not change appreciably with Z and T in the given range.

Table 3 shows the degree of hydrogen bonding, in terms of the average number of hydrogen bonds per molecule, versus temperature for ρ=0.393 g/cm^3 and ρ=0.776 g/cm^3, points respectively below and above the percolation threshold. Once again, the radial distribution functions for these off-Zeno points do not vary significantly within the temperature range shown.

Clustering at the Zeno Point

The lack of any clear structure changes between Zeno and off-Zeno points, combined with the clear change in the degree of hydrogen bonding with temperature and density, suggests that formation and interaction of bonded clusters may provide a better characterization of Zeno-point properties. Using the combined distance-energy criteria, it is simple to construct a connectivity matrix for each sampled configuration from a production run. Using the Markov-chain formulation described in a previous paper, the connectivity matrices can be converted directly to time-averaged cluster size distributions [3]. The cluster size distributions for SPC water at Z=1 appear in Figure 7. The first three distributions, for T=77, 208, and 367 ^{o}C, lie below the percolation threshold of $<n_{hb}>$=1.56. Each of these state points exhibits large-scale clustering of water molecules over time. At 77 ^{o}C, 254 of 256 molecules form one large, bonded cluster. At 208 ^{o}C, clusters ranging in size from 220 to 250 molecules form and dissipate over the simulation timescale of 250 ps, while at 367 ^{o}C clusters ranging from 2 to 210 molecules are nearly equally likely to form. Above the percolation threshold, at T=508, 637, and 766 ^{o}C, the

cluster size distribution clearly indicate a shift to smaller clusters, with monomers, dimers, and clusters up to 10 molecules dominating at the highest temperature.

4. CONCLUSIONS

Molecular simulation using semi-empirical models is effective for modeling the constant-Z contours of pure water. The SPC and SPC/E models, despite their simplicity, do an excellent job approximating the corresponding-states behavior of real water from the Boyle Point to high reduced densities, with each model showing optimal agreement under the conditions for which it was designed.

For SPC water, structural analysis indicates that Z=1.00 state points, from low to high density, may exhibit similar long-range correlation over several molecular lengths, with the magnitude of the correlation being a simple function of average density. This correlation, however, does not uniquely characterize the Zeno point—it is observed to some degree in collections of state points that share similar densities as well as identical compressibilities. Hydrogen bonding studies of these same points show a significant variation in the average number of hydrogen bonds per water molecule among systems with nearly identical local structure, suggesting that the unique properties of Zeno-point systems are derived from the interaction of differently-bonded water clusters. A preliminary examination of these clusters shows how cluster size relates to macroscopic "percolation" of the hydrogen bond network.

Future work in this area should further examine the properties of these water clusters, including the role of tetrahedral and dodoecahedral coordination and the net interactions between the clusters themselves.

ACKNOWLEDGMENTS

Table 1: Equilibrium properties of simulated water at $Z=1.00$ [3].

SPC Model

T (^{o}C)	T_r	P (bar)	Z	ρ (g/cm^3)	ρ_r
77	0.6	1644	1.013	1.011	3.74
208	0.82	2044	1.013	0.914	3.39
367	1.09	2290	1.005	0.776	2.87
508	1.33	2296	0.997	0.643	2.38
637	1.55	2145	1.002	0.513	1.90
766	1.77	1858	0.993	0.393	1.45
1097	2.33	181	1.003	0.029	1.06

SPC/E Model

T (^{o}C)	T_r	P (bar)	Z	ρ (g/cm^3)	ρ_r
77	0.54	1677	1.01	1.034	3.17
208	0.74	2095	1.00	0.949	2.91
367	0.98	2421	1.00	0.825	2.53
508	1.20	2490	1.00	0.698	2.14
637	1.40	2410	1.00	0.580	1.78
766	1.59	2316	1.01	0.483	1.48
1097	2.10	647	1.00	0.103	0.32

Table 2: $\langle n_{hb} \rangle$ vs. T at Z=0.75, 1.00, and 1.25.

	Z=0.75	Z=1.00	Z=1.25
208 °C	2.26	2.31	2.34
367 °C	1.62	1.73	1.80
508 °C	1.09	1.28	1.41
508 °C	0.408	n/a	n/a
597 °C	0.607	n/a	n/a
766 °C	n/a	0.66	0.206

Table 3: Hydrogen bonding vs. T, $\rho=0.776$ and $\rho=0.393$ g/cm^3.

	T (^{o}C)	Z	$<n_{hb}>$
$\rho=0.776$	287	0.606	1.89
	327	0.811	1.80
	367	1.00	1.73
	387	1.08	1.69
	427	1.22	1.62
	467	1.30	1.56
$\rho=0.393$	726	0.957	0.694
	766	1.00	0.656
	806	1.05	0.632
	846	1.06	0.621
	926	1.13	0.583

LIST OF FIGURES

Figure 1: 3D visualizations of the equilibrium configurations of SPC water at $Z=1.00$.

Figure 2: Zeno ($Z=1$) contours for SPC and SPC/E water vs. correlated experimental data[13].

Figure 3: Radial distribution functions for $Z=1$ state points (SPC model) compared to ambient SPC water. Vertical lines denote $r=0.45$ nm and $r=0.6$ nm.

Figure 4: Scaled radial distribution functions for $Z=1$ state points (SPC model) compared to ambient SPC water. Vertical lines denote $r=0.45$ nm and $r=0.6$ nm.

Figure 5: $<n_{hb}>$ vs. T for $Z=1$ state points (SPC model), comparing structural and combined distance-energy techniques. $<n_{hb}>$ for ambient and supercritical SPC water (450 ^{o}C, 250 bar) included for comparison.

Figure 6: $Z=0.75$, 1.00, and 1.25 contours for correlated experimental data [13] and SPC water.

Figure 7: Cluster size distributions for $Z=1$ state points (SPC water).

LIST OF TABLES

Table 1: Equilibrium properties of simulated water at $Z=1.00$ [3].

Table 2: $<n_{hb}>$ vs. T at $Z=0.75$, 1.00, and 1.25.

Table 3: Hydrogen bonding vs. T, $\rho=0.776$ and $\rho=0.393$ g/cm^3.

REFERENCES

[1]   D. Ben-Amotz and D.R. Herschbach, *Israel Journal of Chemistry*. **30**: 59 (1990).

[2]   D. Ben-Amotz and D.R. Herschbach, *J. Phys. Chem.* **94**: 1038 (1990).

[3]   M.C. Kutney, M.T. Reagan, K.A. Smith, J.W. Tester, and D.R. Herschbach, *J. Phys. Chem.* **submitted for publication** (2000).

[4]   J. Xu and D.R. Herschbach, *J. Phys. Chem.* **96**: 2307 (1992).

[5]   I.M. Marrucho and J.F. Ely, *Fluid Phase Eq.* **150-151**: 215 (1998).

[6]   H.J.C. Berendsen, J.P.M. Postma, W.F. van Gunsteren, and J. Hermans. ". in *Jerusalem Symposia on Quantum Chemistry and Biochemistry*. 1981: Reidel.

[7]   Y. Guissani and B. Guillot, *J. Phys. Chem.* **98**: 8221 (1993).

[8]   H.C. Andersen, *J. Computational Phys.* **52**: 24 (1983).

[9]   S. Nosé, *J. Chem. Phys.* **81**: 511 (1984).

[10]   A.G. Kalinichev and J.D. Bass, *Chem. Phys. Lett.* **231**: 301 (1994).

[11]   A.G. Kalinichev. "Computer Simulations of the Properties of Supercritical Water over a Very Wide Range of Temperatures and Pressures". in *4th International Symposium on Supercritical Fluids*. 1997. Sendai, Japan.

[12]   J.J. de Pablo, J.M. Prausnitz, H.J. Strauch, and P.T. Cummings, *J. Chem. Phys.* **93**: 7355 (1991).

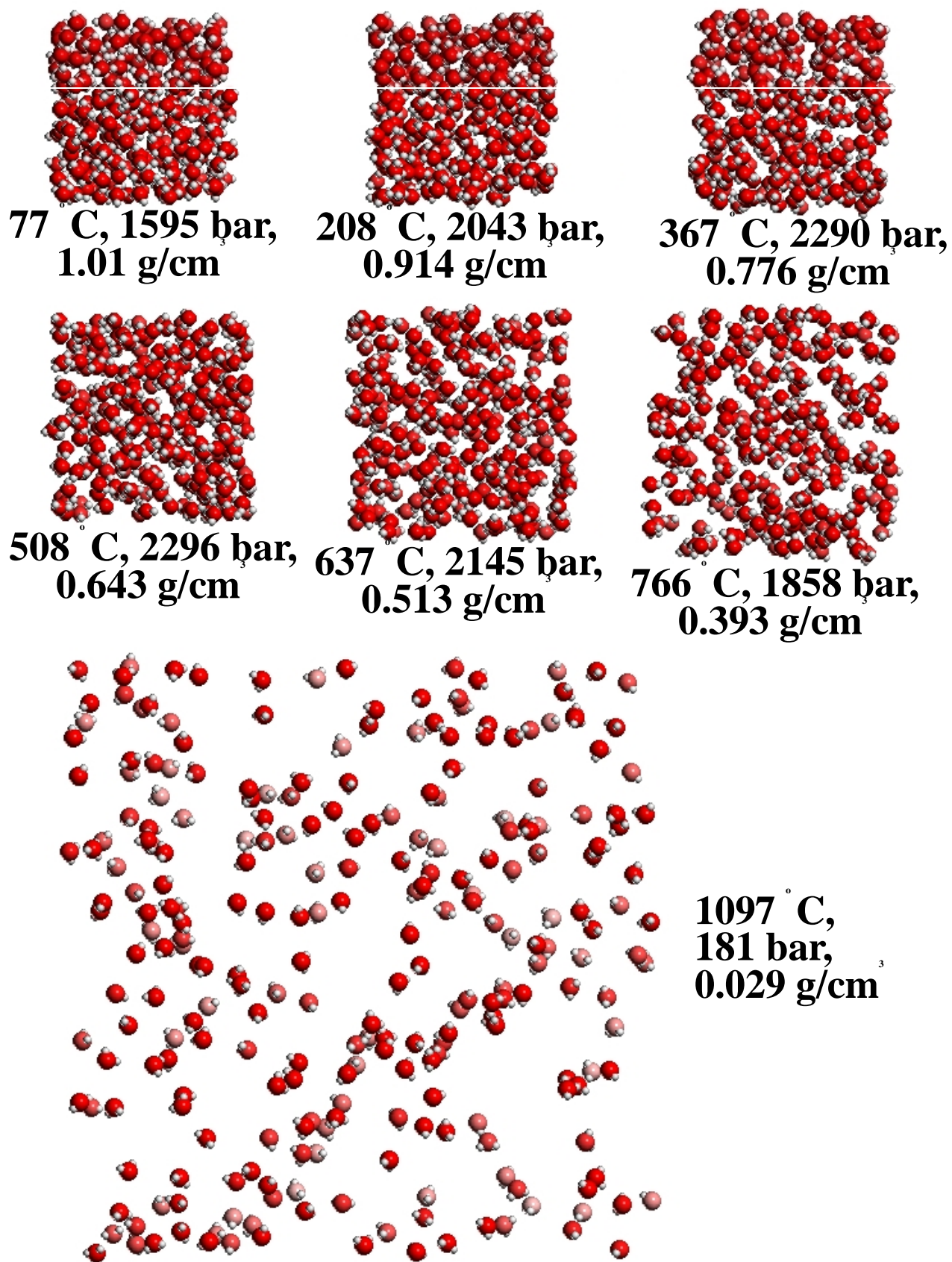[13]   L. Haar and J.S. Gallagher, *NIST Standard Reference Database 10: SteamTables*. 1985, New York.

Figure 1: 3D visualizations of the equilibrium configurations of SPC water at Z=1.00.
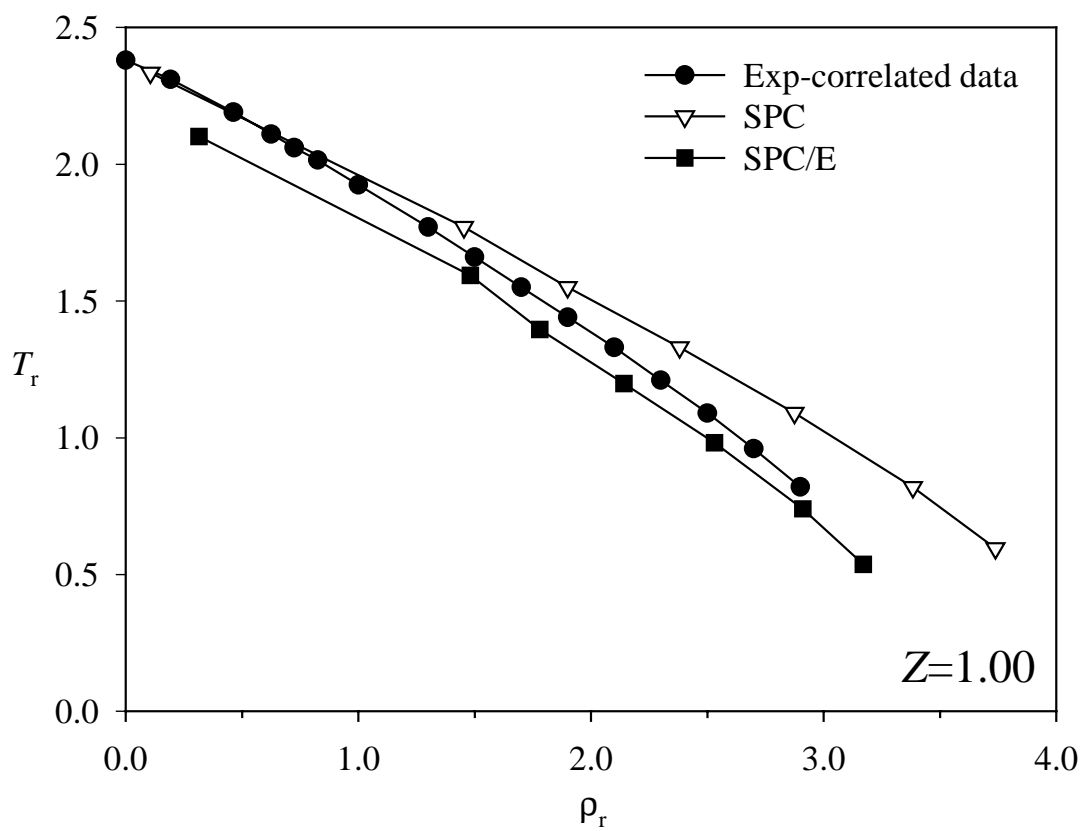
Figure 2: Zeno (*Z*=1) contours for SPC and SPC/E water vs. correlated experimental
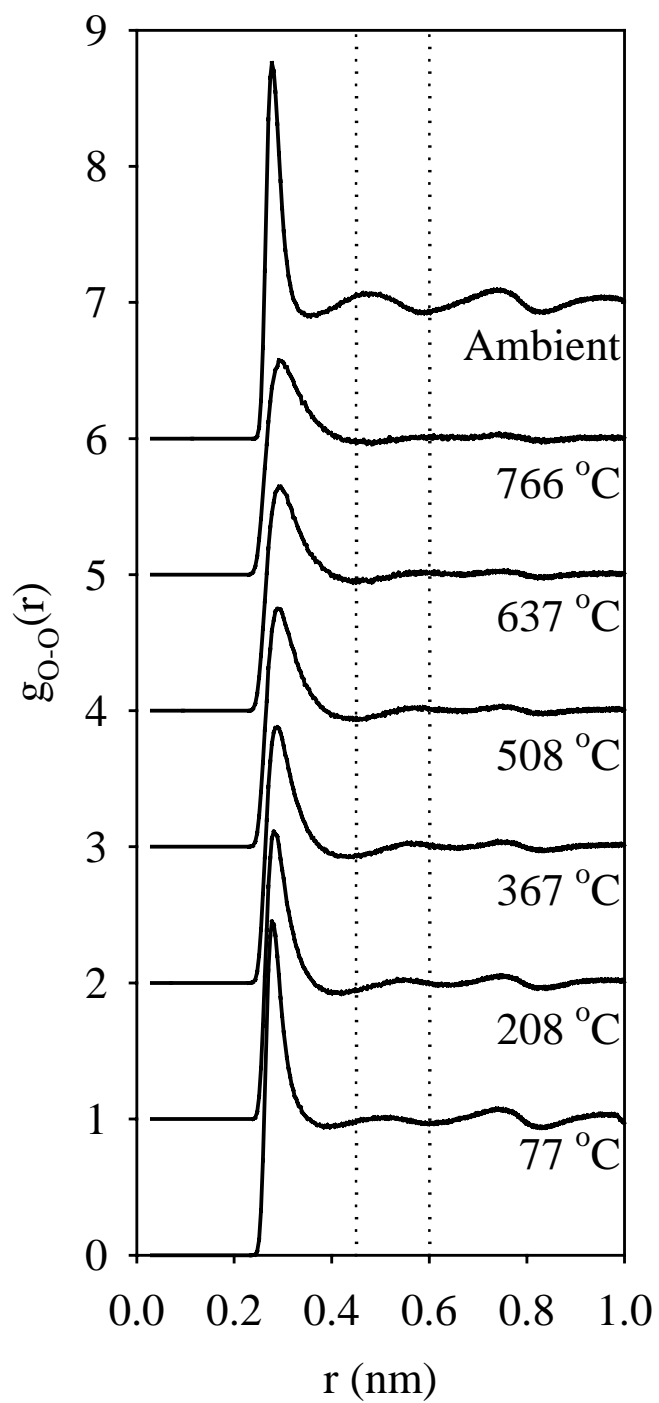
data[13].

Figure 3: Radial distribution functions for $Z=1$ state points (SPC model) compared to ambient SPC water. Vertical lines denote r=0.45 nm and r=0.6 nm.
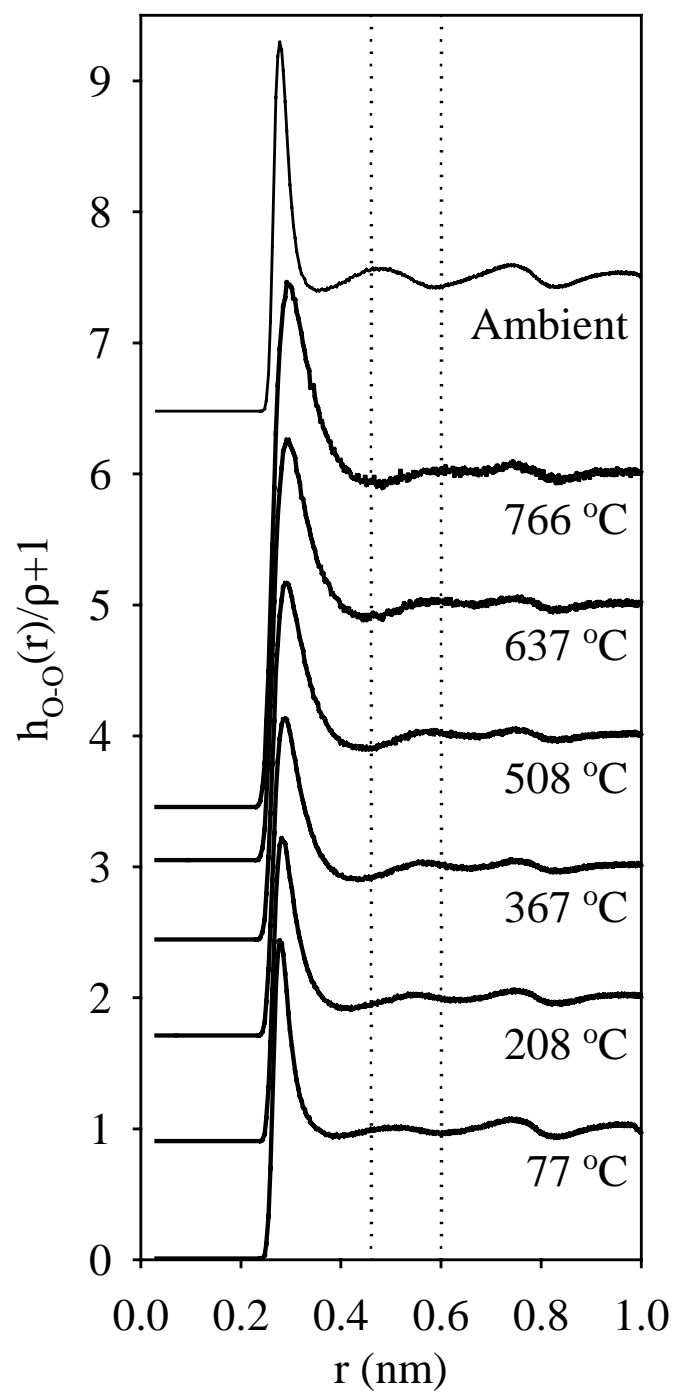
Figure 4: Scaled radial distribution functions for Z=1 state points (SPC model) compared to ambient SPC water. Vertical lines denote r=0.45 nm and r=0.6 nm.
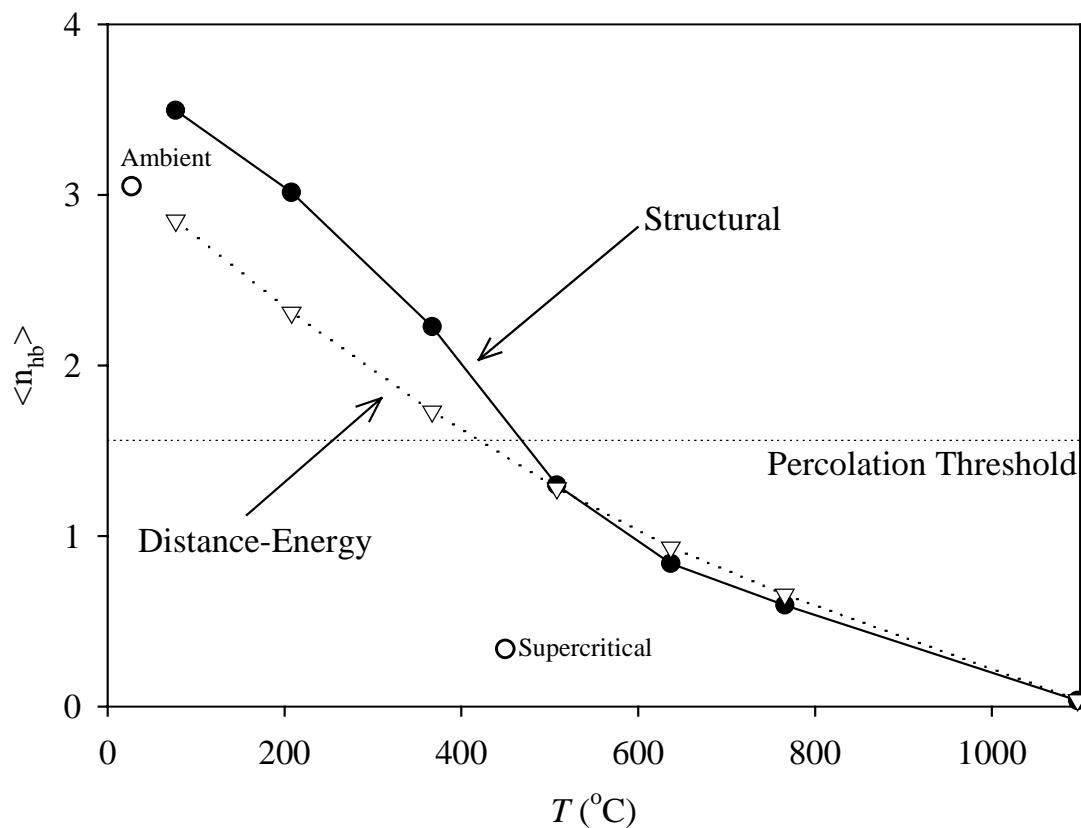
Figure 5: $\langle n_{hb} \rangle$ vs. T for $Z=1$ state points (SPC model), comparing structural and combined distance-energy techniques. $\langle n_{hb} \rangle$ for ambient and supercritical SPC water (450 $^{\circ}$C, 250 bar) included for comparison.
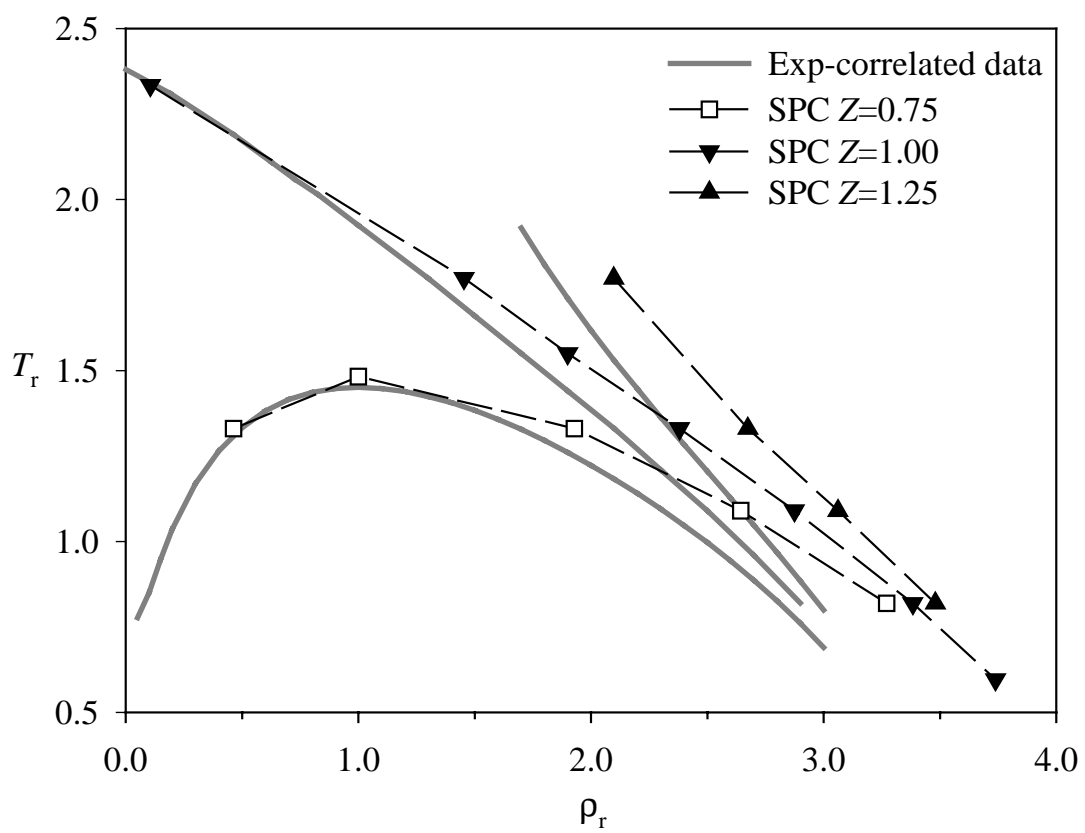
Figure 6: *Z*=0.75, 1.00, and 1.25 contours for correlated experimental data [13] and SPC
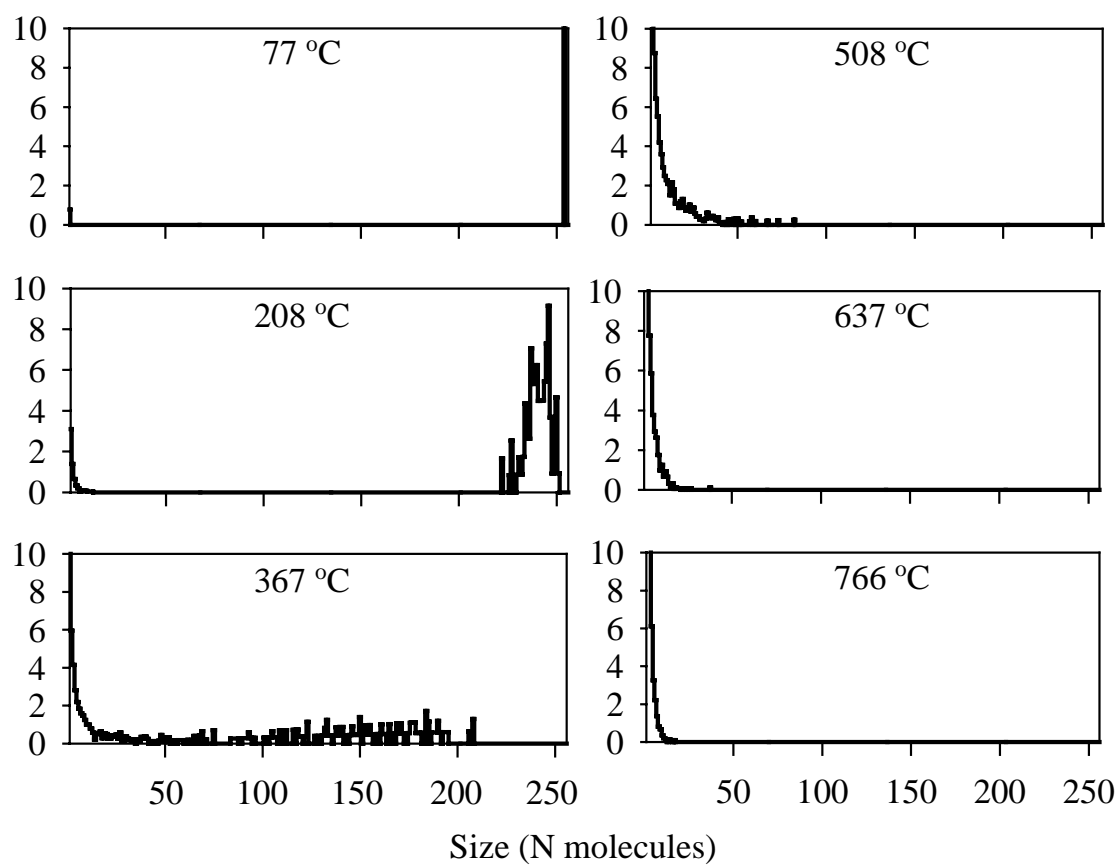
water.

Figure 7: Cluster size distributions for $Z=1$ state points (SPC water).